Total Synthesis of Atrachinenins A and B

Sarah A. French, Christopher J. Sumby, David M. Huang, and Jonathan H. George*

Department of Chemistry, The University of Adelaide, Adelaide, SA 5005, Australia.

ABSTRACT: Inspired by a new biosynthetic hypothesis, we report a biomimetic total synthesis of atrachineins A and B that explains their racemic nature. The synthesis exploits an intermolecular Diels–Alder reaction between a quinone meroterpenoid and *E*-β-ocimene, followed by intramolecular (3+2) cycloaddition and a late-stage aerobic oxidation. Divergent transformations of a simple model system gave several complex polycyclic scaffolds, while also suggesting a structure revision for atrachinenin C.

Stereochemically complex natural products that are isolated as racemates usually originate via non-enzymatic cascade reactions.[1] Their existence can therefore inspire the development of spectacular sequences of predisposed transformations, and the discovery of novel modes of chemical reactivity.[2] For example, atrachinenins A–C (**1**–**3**, Figure 1) are a family of structurally intricate but racemic meroterpenoid natural products[3] recently isolated from the rhizomes of *Atractylodes chinesis*,[4] a plant widely used in traditional Chinese medicine. The most complex member of the family, atrachinenin B (**2**), features a cage-like pentacyclic ring system with seven contiguous stereocenters and a peroxyhemiacetal bridge.

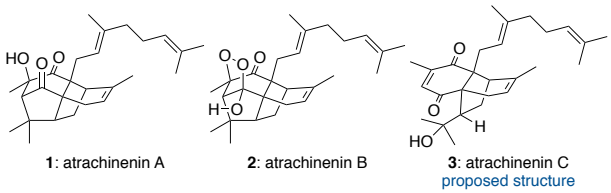

Figure 1. Atrachinenins A–C, a family of complex but racemic meroterpenoids.

In their isolation work, Chen *et al.* suggested a biosynthetic pathway to the atrachinenins that involved an intermolecular Diels–Alder reaction between quinone **4** and a cyclic monoterpene, α-phellandrene, followed by a dyotropic rearrangement and a complicated series of oxidations and cyclizations.[4] Herein, we put forward a much simpler biosynthesis of the atrachinenins (**Scheme 1**), which later serves as the blueprint for their concise total synthesis. First, we propose a racemic, intermolecular Diels–Alder reaction between *E*-β-ocimene (**5**) and quinone **4**,[5] a natural product previously isolated from *Atractylodes lancea*,[6] to give the *endo* adduct **6**. As a readily available monoterpene, *E*-β-ocimene has often been used as a reactive diene in biomimetic Diels–Alder reactions,[7] including as part of complex cascade reactions.[8] Next, we propose enolization of the enedione Diels–Alder adduct **6** at C-5 to give enol **7**, followed by an intramolecular (2+2) photocycloaddition to give cyclobutane **8**. Ring expansion of **8** via an acid or base-catalyzed vinylogous α-ketol rearrangement could then give diketone **9**. Alternatively, we considered that **9** could be formed directly by an acid catalyzed, intramolecular (3+2) cycloaddition of enol **7**. Either way, the C-2-enol of ketone **9** could react with molecular oxygen on its convex face to form the peroxyhemiacetal of atrachinenin B (**2**). Reduction of **2** then gives the tertiary alcohol of atrachinenin A (**1**). We also considered that cyclobutane **8** could undergo oxidative fragmentation to give atrachinenin C (**3**), but this pathway was not supported by later experiments.

Scheme 1. Proposed Biosynthesis of Atrachinenins A and B

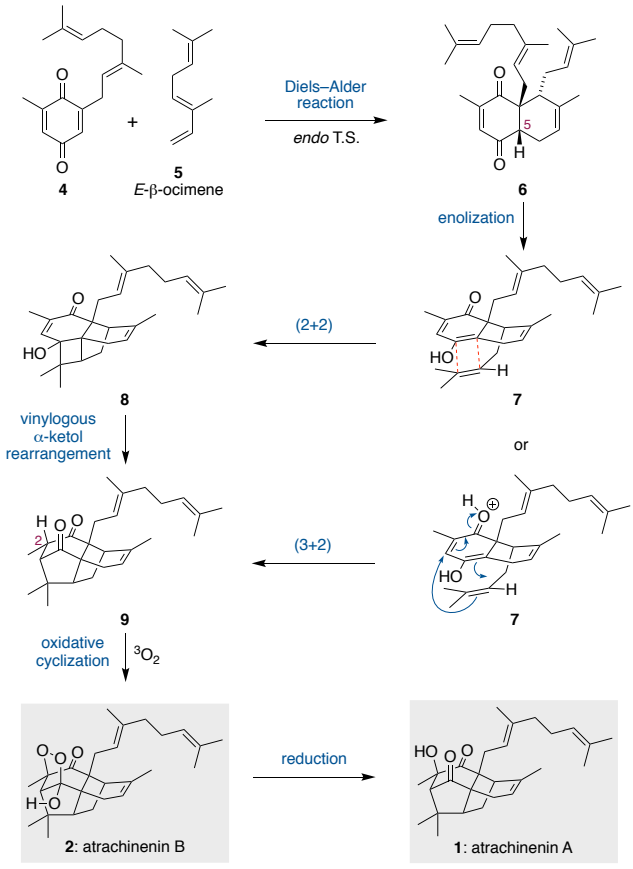

Scheme 2. Intramolecular Cycloadditions of Enedione 12

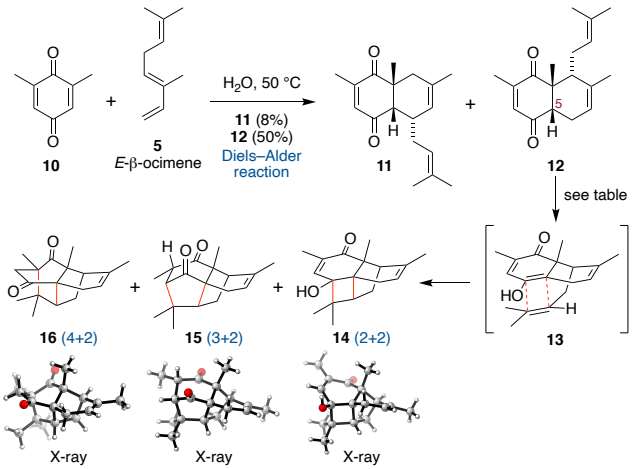

	Conditions	Products
1	NaOMe, MeOH, rt, purple LED	**15** (60%)
2	NaOMe, MeOH, rt, no light	***epi*-12** (69%)
3	$[Ru(bpy)_3]Cl_2$, Et_3N, HCO_2H, MeCN, rt, blue LED	**14** (58%), **15** (14%), **16** (7%)
4	DABCO, MeCN, rt, blue LED	**14** (31%), **15** (17%)
5	CSA, $CHCl_3$, 60 °C	**15** (65%)
6	DABCO, PhMe, 95 °C	**15** (55%)

The ready availability of both *E*-β-ocimene (**5**),[9] and 2,6-dimethylbenzoquinone (**10**) as a simplified analogue of quinone **4**, allowed us to chemically interrogate the proposed biosynthesis of the atrachinenins. First, an on-water catalyzed Diels–Alder reaction[10] between **5** and **10** gave the major *endo* adduct **12** in good yield, which was easily separated from the minor *endo* regioisomer **11** by column chromatography (**Scheme 2**).[11] Exposure of a solution of **12** in NaOMe/MeOH to UV light (λ_{max} = 365 nm) gave a complex mixture of products, but the (3+2) cycloadduct **15** was detected in ^{1}H NMR spectra of the crude reaction mixture. We propose a mechanism involving (2+2) photocycloaddition of enol or enolate **13** via a triplet excited state, followed by base catalyzed ring expansion of **14** via a vinylogous α-ketol rearrangement – a sequence with some analogy to the De Mayo reaction.[12] Measurement of the UV-vis absorption spectrum of **13** in NaOMe/MeOH revealed broad absorption in the range 350 – 440 nm. We therefore conducted a more selective photocycloaddtion using a purple LED (λ_{max} = 405 nm, 390 – 425 nm) as the light source, forming **15** in 60% isolated yield (entry 1).[13] In the dark, NaOMe in MeOH merely epimerized **12** at C-5 (entry 2). Next we explored visible light photoredox catalysis inspired by Yoon's photocatalyzed (2+2) cycloaddition of dienones.[14] Exposure of enedione **12** to standard photoreductive conditions (10 mol% $[Ru(bpy)_3]Cl_2$, Et_3N, HCO_2H, MeCN, blue LED, room temperature) formed the (2+2) cycloadduct **14** as the major product, alongside **15** and the (4+2) cycloadduct **16** as a minor by-product (entry 3). However, some product formation was also observed in the absence of a photocatalyst (entry 4), indicating that the blue LED (λ_{max} = 450 nm, 420 – 470 nm) was capable of mediating the photocycloaddition of **12** to some extent. A cycloaddition mechanism involving electron transfer by the photocatalyst to enol **13** is therefore unlikely. However, use of the more powerful photocatalyst $(Ir[Me(Me)ppy]_2(dtbpy))PF_6$ resulted in reduction of enedione **12** to give a saturated diketone product via a radical anion intermediate (see the Supporting Information).[15] Finally, and in line with our alternative biosynthetic proposal outlined in **Scheme 1**, enedione **12** also undergoes acid and base catalyzed, intramolecular (3+2) cycloadditions to give **15** on heating with catalytic CSA in $CHCl_3$ at 60 °C (entry 5), or with catalytic DABCO in PhMe at 95 °C (entry 6).

These experimental results show that formation of the desired (3+2) cycloadduct **15** from **12** is highly predisposed to occur under a variety of photochemical and thermal conditions. To gain further insight into the mechanism of these cycloadditions, molecular geometries and energies of proposed intermediates were calculated using density function theory (DFT) (see the Supporting Information for full details).[16] Our calculations predict the lowest energy pathway ($\Delta G^{\ddagger}$ = 75.3 kJ/mol) is an acid catalyzed (3+2) cycloaddition of enol **13** that is concerted but asynchronous. An alternative acid catalyzed (2+2) cycloaddition of **13** to give **14** is slightly less favored ($\Delta G^{\ddagger}$ = 85.0 kJ/mol), but the subsequent vinylogous α-ketol rearrangement to give **15** is facile ($\Delta G^{\ddagger}$ = 34.7 kJ/mol). For the photochemical cycloadditions, our calculations support a mechanism involving photoexcitation of **13** to a triplet state biradical, followed by a stepwise (2+2) cycloaddition to give **14**, with a favorable base catalyzed vinylogous α-ketol rearrangement to then give **15** ($\Delta G^{\ddagger}$ = 26.7 kJ/mol).

Scheme 3. Divergent Synthesis of Atrachinenin Analogues From Cyclobutane 14

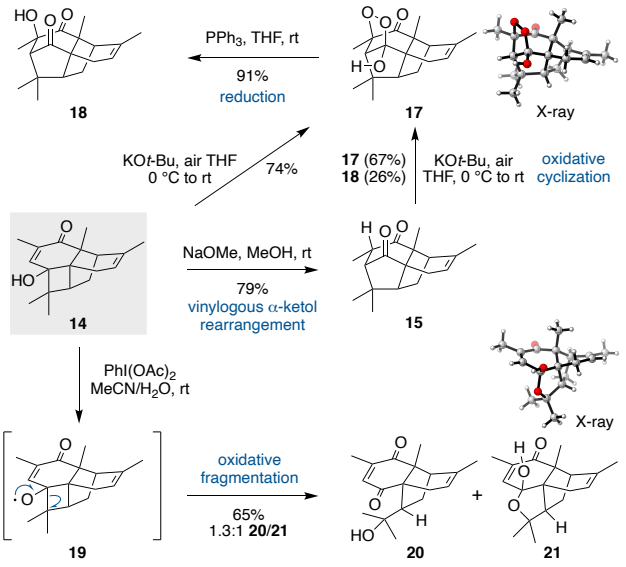

Next, we investigated the rearrangement and oxidation of cyclobutane **14** to give synthetic analogues of atrachinenins A, B and C (**Scheme 3**). As predicted by our DFT study, the (2+2) cycloadduct **14** undergoes facile ring expansion via a vinylogous α-ketol rearrangement[17] under either acid or base catalysis to give **15** in high yield, *e.g.* with catalytic camphorsulfonic acid (CSA) in $CHCl_3$, or NaOMe in MeOH. Addition of KO*t*-Bu to a solution of **15** in THF open to air then formed the cyclic peroxyhemiacetal **17** (an analogue of atrachinenin B) in good yield via an α-hydroperoxide intermediate,[18] alongside tertiary alcohol **18** as a minor product. The atrachinenin A

analogue **18** was then more efficiently accessed by reduction of **17** with PPh_3. Under basic conditions, the vinylogous α-ketol rearrangement was combined with the aerobic oxidation step to directly convert **14** to **17** in high yield. Finally, oxidation of **14** with $PhI(OAc)_2$ gave an interconverting mixture of the atrachinenin C analogue **20** alongside its ring closed cyclic hemiacetal **21** (1.3:1 in $CDCl_3$) via C–C cleavage of the alkoxy radical **19**.[19] X-ray analysis of crystals of **21** proved its cyclic structure, which reverted back to a mixture of **20** and **21** on dissolution in $CDCl_3$. This ketone-hemiacetal equilibrium contrasts with the natural product atrachinenin C, which is proposed to exist solely as structure **3**. ^1H and ^{13}C NMR data for **3** also differs significantly from that observed for model compound **20**, particularly at Me-15, Me-16, H-12 and H-6.[4]

Scheme 4. Proposed Structure Revision of Atrachinenin C

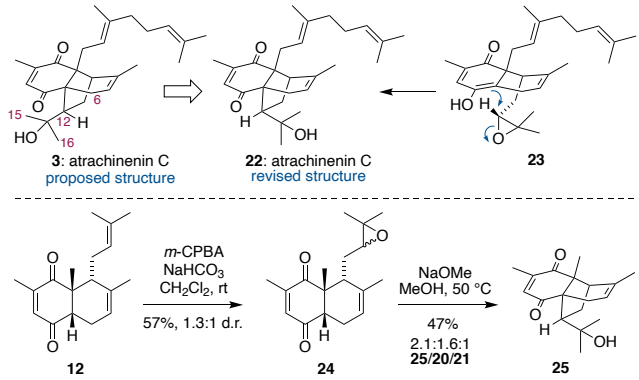

We therefore propose that the structure of atrachinenin C was misassigned at the C-12 stereocentre and that its true structure is C-12-epimer **22**, which could arise biosynthetically via *5-exo-trig* cyclization of epoxide **23** (**Scheme 4**). The original assignment of **3** was based on a claimed NOE interaction between H-12 and H-6α; however, the overlap between H-12 and H-6β signals in the ^1H NMR spectrum renders this correlation unclear. Furthermore, based on our synthetic work we predict that the proposed tricyclic diketone structure **3** should be in equilibrium with its tetracyclic hemiacetal form. Final support in favor of our structure revision was obtained through the synthesis of the atrachinenin C analogue **25** via base catalyzed cyclization of epoxide **24**, with NMR data for **25** in excellent agreement with natural atrachinenin C (see the Supporting Information for full details).

Enedione **12** also undergoes three further modes of acid promoted cyclization (**Scheme 5**). Firstly, when the acid catalyzed (3+2) cycloaddition of **12** was conducted in an open flask, the intermediate product **15** underwent further aerobic oxidation to give cyclic peroxyhemiacetal **17** in good yield. This compound is unstable on heating (or exposure to UV light), rearranging to give lactone-hemiacetal **26** in high yield at 80 °C in PhMe. We propose a mechanism of homolytic O–O bond cleavage to give a biradical, followed by a concerted 1,2-methyl shift and C–C fragmentation to give a carboxylic acid, which then cyclizes to give **26**. A related, thermal fragmentation of monocyclic 3-hydroxy-1,2-dioxoloanes to give carboxylic acid and ketone products has been reported.[20] Alternatively, treatment of **12** with 6 M HCl in THF gave the tetracyclic product **27** via an intramolecular (5+2) cycloaddition. Under these strongly acidic, aqueous conditions, we propose that protonation of the C-1 carbonyl group of enol **13** could trigger a Prins reaction with the pendant prenyl group to give a tertiary carbocation. Interception of this carbocation by the C-5 enol could then form **27** via a stepwise, formal (5+2) cycloaddition. Finally, reaction of **12** with BF_3•Et_2O at –78 °C gave tertiary alcohol **28** via a type I intramolecular carbonyl-ene reaction without enolization at C-5.[21]

Scheme 5. Further Reactions of Enedione 12

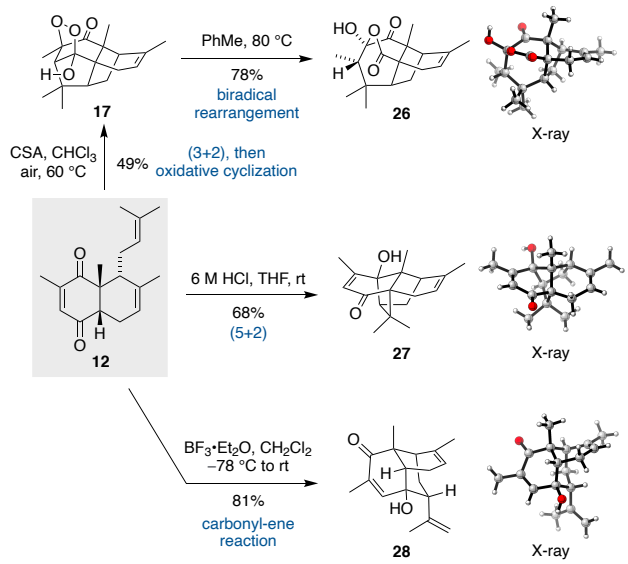

After these extensive model studies, we were armed with enough knowledge of the diverse chemistry of quinone–ocimene Diels–Alder adducts to attempt a total synthesis of the atrachinenins. This required access to the naturally occurring quinone **4**, which was achieved in high yield by *C*-geranylation of 4-methoxy-2-methylphenol (**29**) to give **30**, followed by oxidation with ceric ammonium nitrate (CAN) (**Scheme 6**). Next, use of a high concentration of $LiClO_4$ in Et_2O, Grieco's conditions for rate accelerated Diels–Alder reactions,[22] enabled an efficient union between **4** and *E*-β-ocimene (**5**) to give a mixture of all four possible *endo* adducts **6**, **31**, **32** and **33**. The on-water Diels–Alder reaction between **4** and **5** gave a slightly lower conversion in this case. Monitoring the product mixture using an internal NMR standard showed formation of **6** and **31** as the major products (both 36%) alongside **32** and **33** (both 7%), which is consistent with our model system. From this complex mixture, the desired adduct **6** was purified in 24% overall yield by careful silver nitrate chromatography.[23] Intramolecular (3+2) cycloaddition of **6** was also more challenging than the model system due to the proclivity of the geranyl substituent to migrate from C-10 to C-2, forming **34** as the major product under all photochemical and most thermal conditions. The mechanism of this undesired transformation probably involves successive retro-Claisen and Claisen rearrangements of the geranyl side chain of **6** around the cyclohexenedione ring system since **34** was formed as a 1.3:1 mixture of *E* and *Z* stereoisomers.[24] Furthermore, a simplified analogue of **6** with an allyl group at C-10 underwent a single retro-Claisen rearrangement to give an aromatic allyl ether product (see the Supporting Information for details). On further heating (or standing at room temperature for several days), **34** underwent a Cope rearrangement and retro-ene reaction to give the aromatized by-product **35**.

Scheme 6. Total Synthesis of Atrachinenins A and B

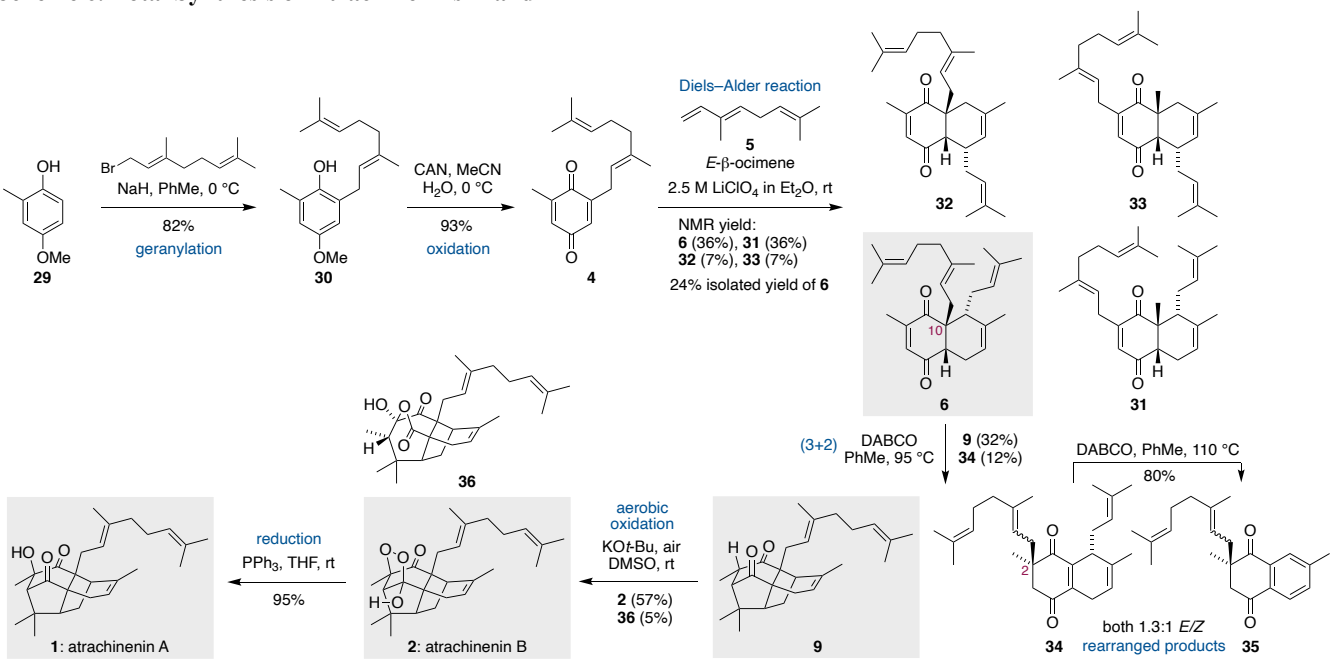

Despite the undesired geranyl migration under photochemical conditions, careful control of a thermal reaction with catalytic DABCO allowed formation of the desired (3+2) cycloadduct **9** in 32% yield, with higher temperatures favoring **34** and **35**. Unlike the model system, aerobic oxidation of **8** with KO*t*-Bu in THF gave a complex mixture of products but switching the solvent to DMSO gave atrachinenin B (**2**) in 57% yield, alongside lactone-hemiacetal **36** formed by rearrangement of **2**. Finally, atrachinenin B (**2**) was reduced with PPh_3 to provide atrachinenin A (**1**) in high yield. Spectroscopic data for synthetic **1** and **2** matched those of the natural products, which were assigned by NMR and X-ray studies.[4]

In summary, we have achieved concise total syntheses of atrachinenins A and B based on a novel biosynthetic hypothesis that rationalizes their racemic nature. Our synthesis explores the predisposed reactivity of Diels-Alder adducts formed between simple quinone and terpene building blocks, with remarkable structural diversity resulting from subsequent cycloadditions, carbonyl-ene reactions and sigmatropic rearrangements. Although the use of unprotected intermediates in a bold, biomimetic strategy leads to some unselective steps, the synthesis and characterization of several biosynthetic intermediates and by-products could facilitate their future isolation as natural products from *Atractylodes* plants.[25] We provide experimental and computational evidence that the polycylic ring system of atrachinenins A and B could arise from either (2+2) or (3+2) intramolecular cycloadditions, while our work also signals that a structure revision is necessary for atrachinenin C.

ASSOCIATED CONTENT

Supporting Information

The Supporting Information is available free of charge on the ACS Publications website.

Experimental procedures, DFT calculations, spectroscopic data and copies of NMR spectra for all compounds (PDF)

Accession Codes

CCDC 2205935−2205940 and 2219400−2219402 contain the supplementary crystallographic data for this paper. These data can be obtained free of charge via www.ccdc.cam.ac.uk/data_request/cif, or by emailing data_request@ccdc.cam.ac.uk, or by contacting The Cambridge Crystallographic Data Centre, 12 Union Road, Cambridge CB2 1EZ, UK; fax: +44 1223 336033.

AUTHOR INFORMATION

Corresponding Author

*jonathan.george@adelaide.edu.au

ACKNOWLEDGMENT

This work was supported by the Australian Research Council (DP200102964).

REFERENCES

(1) Novak, A. J. E.; Trauner, D. Reflections on Racemic Natural Products. *Trends Chem.* **2020**, *2*, 1052.

(2) For selected biomimetic syntheses of stereochemically complex but racemic natural products, see: (a) Drew, S. L.; Lawrence, A. L.; Sherburn, M. S. Total Synthesis of Kingianins A, D, and F. *Angew. Chem. Int. Ed.* **2013**, *52*, 4221. (b) Lam, H. C.; Spence, J. T. J.; George, J. H. Biomimetic Total Synthesis of Hyperjapones A–E and Hyperjaponols A and C. *Angew. Chem. Int. Ed.* **2016**, *55*, 10368. (c) Novak, A. J. E.; Grigglestone, C. E.; Trauner, D. A Biomimetic Synthesis Elucidates the Origin of Preuisolactone A. *J. Am. Chem. Soc.* **2019**, *141*, 15515.

(3) For reviews on the biosynthesis and biomimetic synthesis of meroterpenoids, see: (a) Geris, R.; Simpson, T. J. Meroterpenoids produced by fungi. *Nat. Prod. Rep.* **2009**, *26*, 1063. (b) Matsuda, Y.; Abe, I. Biosynthesis of fungal meroterpenoids. *Nat. Prod. Rep.* **2016**, *33*, 26. (c) Murray, L. A. M.; McKinnie, S. M. K.; Moore, B. S.; George, J. H. Meroterpenoid natural products from *Streptomyces* bacteria – the evolution of chemoenzymatic syntheses. *Nat. Prod. Rep.* **2020**, *37*, 1334. (d) George, J. H. Biomimetic Dearomatization Strategies in the Total Synthesis of Meroterpenoid Natural Products. *Acc. Chem. Res.* **2021**, *54*, 1843. (e) Han, J.; Jiang, L.; Zhang, L.;

Quinn, R. J.; Liu, X.; Feng, Y. Peculiarities of meroterpenoids and their bioproduction. *Appl. Microbiol. Biotechnol.* **2021**, *105*, 3987.
(4) Chen, F.-L.; Liu, D.-L.; Fu, J.; Yang, J.; Bai, L.-P.; Zhang, W.; Jiang, Z.-H.; Zhu, G.-Y. (±)-Atrachinenins A-C, Three Pairs of Caged C_{27} Meroterpenoids from the Rhizomes of *Atractylodes chinensis*. *Chin. J. Chem.* **2022**, *40*, 460.
(5) For a review of quinones as dienophiles in the Diels–Alder reaction, see: Nawrat, C. C.; Moody, C. J. Quinones as Dienophiles in the Diels–Alder Reaction: History and Applications in Total Synthesis. *Angew. Chem. Int. Ed.* **2014**, *53*, 2056.
(6) (a) Resch, M.; Steigel, A.; Chen, Z.-L.; Bauer, R. 5-Lipoxygenase and cyclooxygenase-1 inhibitory active compounds from *Atractylodes lancea*. *J. Nat. Prod.* **1998**, *61*, 347. (b) Jeong, D.; Dong, G.-Z.; Lee, H. J.; Ryu, J.-H. Anti-Inflammatory Compounds from *Atractylodes macrocephala*. *Molecules* **2019**, *24*, 1859. Also isolated from a marine alga: (c) Capon, R. J.; Ghisalberti, E. L.; Jefferies, P. R. Isoprenoid dihydroquinones from a brown alga, *Cystophora* sp. *Phytochemistry* **1981**, *20*, 2598.
(7) (a) Cong, H.; Becker, C. F.; Elliott, S. J.; Grinstaff, M. W.; Porco, J. A. Jr. Silver Nanoparticle-Catalyzed Diels−Alder Cycloadditions of 2'-Hydroxychalcones. *J. Am. Chem. Soc.* **2010**, *132*, 7514. (b) Homer, J. A.; De Silvestro, I.; Matheson, E. J.; Stuart, J. T.; Lawrence, A. L. Enantioselective *para*-Claisen Rearrangement for the Synthesis of *Illicium*-Derived Prenylated Phenylpropanoids. *Org. Lett.* **2021**, *23*, 3248.
(8) (a) Majetich, G.; Zhang, Y. Concise Synthesis of (±)-Perovskone. *J. Am. Chem. Soc.* **1994**, *116*, 4979. (b) Yuan, C.; Du, B.; Yang, L.; Liu, B. Bioinspired Total Synthesis of Bolivianine: A Diels–Alder/Intramolecular Hetero-Diels–Alder Cascade Approach. *J. Am. Chem. Soc.* **2013**, *135*, 9291. (c) Yang, B.; Wen, G.; Zhang, Q.; Hou, M.; He, H.; Gao, S. Asymmetric Total Synthesis and Biosynthetic Implications of Perovskones, Hydrangenone, and Hydrangenone B. *J. Am. Chem. Soc.* **2021**, *143*, 6370. (d) Franov, L. J.; Hart, J. D.; Pullella, G. A.; Sumby, C. J.; George, J. H. Bioinspired Total Synthesis of Erectones A and B, and the Revised Structure of Hyperelodione D. *Angew. Chem. Int. Ed.* **2022**, *61*, e202200420.
(9) We used a commercially available 2:1 mixture of *E*- and *Z*-isomers of β-ocimene (the *Z*-isomer did not undergo a Diels–Alder reaction with quinone **10**).
(10) For seminal studies on the Diels–Alder reaction in water, see: (a) Breslow, R. Hydrophobic effects on simple organic reactions in water. *Acc. Chem. Res.* **1991**, *24*, 160. (b) Narayan, S.; Muldoon, J.; Finn, M. G.; Fokin, V. V.; Kolb, H. C.; Sharpless, K. B. "On Water": Unique Reactivity of Organic Compounds in Aqueous Suspension. *Angew. Chem. Int. Ed.* **2005**, *44*, 3275. For a recent example in a biomimetic total synthesis, see: (c) Lam, H. C.; Pepper, H. P.; Sumby, C. J.; George, J. H. Biomimetic Total Synthesis of (±)-Verrubenzospirolactone. *Angew. Chem. Int. Ed.* **2017**, *56*, 8532.
(11) For intermolecular quinone Diels–Alder reactions with similar regioselectivity/stereoselectivity, see: (a) Kerkar, B.; Khac, D. D.; Fetizon, M.; Guir, F. An Angular Hydroxylation Route to Taxanes: Facile Access to the Bridged AB Ring System of Taxol. *Tetrahedron Lett.* **1997**, *38*, 3223. (b) Donatoni, M. C.; Junior, G. A. B.; de Oliveira, K. T.; Ando, R. A.; Brocksom, T. J.; Dos Santos, A. A. Solvent-free Diels–Alder reactions catalyzed by $FeCl_3$ on Aerosil silica. *Tetrahedron* **2014**, *70*, 3231.
(12) For reviews of the De Mayo reaction, see: (a) Kaŕkaš, M. D.; Porco, J. A., Jr.; Stephenson, C. R. J. Photochemical Approaches to Complex Chemotypes: Applications in Natural Product Synthesis. *Chem. Rev.* **2016**, *116*, 9683. (b) Poplata, S.; Tröster, A.; Zou, Y.-Q.; Bach, T. Recent Advances in the Synthesis of Cyclobutanes by Olefin [2 + 2] Photocycloaddition Reactions. *Chem. Rev.* 2**016**, *116*, 9748.
(13) For a recent use of purple LED in biomimetic synthesis, see: Wen, S.; Boyce, J. H.; Kandappa, S. K.; Sivaguru, J.; Porco, J. A., Jr. Regiodivergent Photocyclization of Dearomatized Acylphloroglucinols: Asymmetric Syntheses of (−)-Nemorosone and (−)-6-*epi*-Garcimultiflorone A. *J. Am. Chem. Soc.* **2019**, *141*, 11315.
(14) (a) Ischay, M. A.; Anzovino, M. E.; Du, J.; Yoon, T. P. Efficient Visible Light Photocatalysis of [2+2] Enone Cycloadditions. *J. Am. Chem. Soc.* **2008**, *130*, 12886. (b) Du, J.; Ruiz Espelt, L.; Guzei, I. A.; Yoon, T. P. Photocatalytic reductive cyclizations of enones: Divergent reactivity of photogenerated radical and radical anion intermediates. *Chem. Sci.* **2011**, *2*, 2115.
(15) Pac, C.; Ihama, M.; Yasuda, M.; Miyauchi, Y.; Sakurai, H. $Ru(bpy)_3^{2+}$-Mediated Photoreduction of Olefins with 1-Benzyl-1,4-dihydronicotinamide: A Mechanistic Probe for Electron-Transfer Reactions of NAD(P)H-Model Compounds. *J. Am. Chem. Soc.* **1981**, *103*, 6495.
(16) Molecular geometries and energies of proposed intermediates were calculated by density function theory (DFT) using the ORCA quantum chemistry software package (version 5.0.3.). Geometries were optimized in the gas phase using the ωB97X-D3 functional and def2-SVP basis set. Transition states were obtained using a combination of the climbing image nudged elastic band method and an eigenvector-following optimization of the climbing image. See the Supporting Information for full details. (a) Neese, F. The ORCA program system. *WIREs Comput. Mol. Sci.* **2012**, *2*, 73. (b) Neese, F.; Wennmohs, F.; Becker, U.; Riplinger, C. The ORCA quantum chemistry program package. *J. Chem. Phys.* **2020**, *152*, 224108. (c) Lin. Y.-S.; Li, G.-D.; Mao, S.-P.; Chai, J.-D. Long-Range Corrected Hybrid Density Functionals with Improved Dispersion Corrections. *J. Chem. Theory Comput.* **2013**, *9*, 263. (d) Weigand, F.; Ahlrichs, R. Balanced basis sets of split valence, triple zeta valence and quadruple zeta valence quality for H to Rn: Design and assessment of accuracy. *Phys. Chem. Chem. Phys.* **2005**, *7*, 3297. (e) Ásgeirsson, V.; Birgisson, B. O.; Bjornsson, R.; Becker, U.; Neese, F.; Riplinger, C.; Jónsson, H. Nudged Elastic Band Method for Molecular Reactions Using Energy-Weighted Springs Combined with Eigenvector Following. *J. Chem. Theory Comput.* **2021**, *17*, 4929.
(17) Zhang, E.; Fan, C.-A.; Tu, Y.-Q.; Zhang, F.-M.; Song, Y.-L. Organocatalytic Asymmetric Vinylogous α-Ketol Rearrangement: Enantioselective Construction of Chiral All-Carbon Quaternary Stereocenters in Spirocyclic Diketones via Semipinacol-Type 1,2-Carbon Migration. *J. Am. Chem. Soc.* **2009**, *131*, 14626.
(18) (a) Liang, Y.-F.; Jiao, N. Highly Efficient C–H Hydroxylation of Carbonyl Compounds with Oxygen under Mild Conditions. *Angew. Chem. Int. Ed.* **2014**, *53*, 548. (b) Novkovic, L.; Trmcic, M.; Bihelovic, F.; Zlatar, M.; Matovic, R.; Saicic, R. N. Synthesis of endoperoxides by domino reactions of ketones and molecular oxygen. *RSC Adv.* **2015**, *5*, 99577.
(19) Kinouchi, H.; Sugimoto, K.; Yamaoka, Y; Takikawa, H.; Takasu, K. Oxidative β-Cleavage of Fused Cyclobutanols Leading to Hydrofuran-Fused Polycyclic Aromatic Compounds. *J. Org. Chem.* **2021**, *86*, 12615.
(20) (a) Baumstark, A. L.; Vasquez, P. C. Thermolysis of pentasubstituted 3-hydroxy-1 2-dioxolanes. *J. Heterocyclic. Chem.* **1992**, *29*, 1781. (b) Baumstark, A. L.; Vasquez, P. C.; Chen, Y.-X. Synthesis and Thermolysis of Ketal Derivatives of 3-Hydroxy-l,2-dioxolanes. *J. Org. Chem.* **1994**, *59*, 6692.
(21) Snider, B. B. Prins Reactions and Carbonyl, Imine, and Thiocarbonyl Ene Reactions. In Comprehensive Organic Synthesis, Vol. 2, 2nd ed.; Molander, G. A.; Knochel, P., Eds.; Oxford, Elsevier, **2014**; ch. 2.03, pp. 148–191.
(22) Grieco, P. A.; Nunes, J. J.; Gaul, M. D. Dramatic Rate Accelerations of Diels–Alder Reactions in 5 M Lithium Perchlorate-Diethyl Ether: The Cantharidin Problem Reexamined. *J. Am. Chem. Soc.* **1990**, *112*, 4595.
(23) Williams, C. M.; Mander, L. N. Chromatography with silver nitrate. *Tetrahedron* **2001**, *57*, 425.
(24) For some similar rearrangements, see: (a) Miller, B. Too many rearrangements of cyclohexadienones. *Acc. Chem. Res.* **1975**, *8*, 245. (b) Fujimoto, Y.; Takahashi, K.; Kobayashi, R.; Fukaya, H.; Yanai, H.; Matsumoto, T. Anion-Accelerated Aromatic Oxy-Cope Rearrangement in Geranylation/Nerylation of Xanthone: Stereochemical Insights and Synthesis of Fuscaxanthone. *Synlett* **2020**, *31*, 1378.
(25) Hetzler, B. E.; Trauner, D. Lawrence, A. L. Natural product anticipation through synthesis. *Nat. Rev. Chem.* **2022**, *6*, 170.

Graphical abstract: